ACS APPLIED BIO MATERIALS
Cite This: ACS Appl. Bio Mater. 2019, 2, 1509−1517
Article
www.acsabm.org

Jammed Polyelectrolyte Microgels for 3D Cell Culture Applications: Rheological Behavior with Added Salts

Christopher S. O'Bryan,[†] Christopher P. Kabb,[‡] Brent S. Sumerlin,[§] and Thomas E. Angelini*[,†,§,∥,⊥]

[†]Department of Mechanical & Aerospace Engineering, Herbert Wertheim College of Engineering, University of Florida, Gainesville, Florida 32611, United States

[‡]George & Josephine Butler Polymer Research Laboratory, Center for Macromolecular Science & Engineering, Department of Chemistry, University of Florida, Gainesville, Florida 32611, United States

[§]J. Crayton Pruitt Family Department of Biomedical Engineering, Herbert Wertheim College of Engineering, University of Florida, Gainesville, Florida 32611, United States

[∥]Institute for Cell & Tissue Science and Engineering, University of Florida, Gainesville, Florida 32611, United States

[⊥]Department of Materials Science and Engineering, Herbert Wertheim College of Engineering, University of Florida, Gainesville, Florida 32611, United States

Supporting Information

ABSTRACT: The yielding and jamming behaviors of packed granular-scale microgels enable their use as a support medium for 3D printing stable shapes made from liquid phases; under low levels of applied stress, jammed microgel packs behave like elastic solids and provide support to spatially patterned fluid structures. When swollen in cell growth media, these microgels constitute a biomaterial for bioprinting and 3D cell culture applications. However, interactions between polyelectrolytes commonly used in microgels and multivalent ions present in cell growth media may lead to drastic and adverse changes in rheological behavior or cell performance. To elucidate these interactions, we design polyelectrolyte microgels with anionic, cationic, and zwitterionic charged species and investigate their rheological behaviors in $CaCl_2$ solutions. We find the rheological behavior of anionic and cationic microgels follow polyelectrolyte scaling laws near jamming concentrations; the rheological properties of zwitterionic microgels become independent of $CaCl_2$ at high concentrations. We explore the potential application of these microgels as biomaterials for 3D cell culture through studies of short-term cell viability, population growth, and metabolic activity. We find that the short-term viability of cells cultured in polyelectrolytes is highly dependent on the chemical composition of the system. In addition, we find that anionic and zwitterionic microgels have minimal effects on the short-term viability and metabolic activity of cells cultured in microgel environments across a wide range of rheological properties.

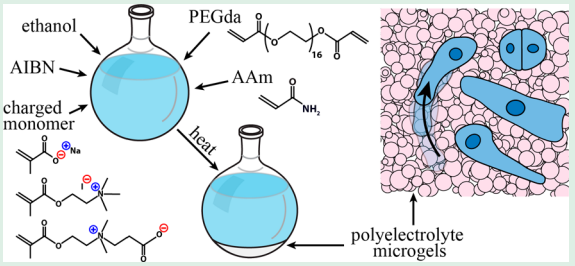

KEYWORDS: *microgels, polyelectrolytes, multivalent ions, 3D cell culture, bioprinting*

INTRODUCTION

Microscale hydrogel particles, commonly called microgels, can be packed together to form jammed solids that exhibit dominantly elastic responses to small levels of shear deformation.[1−4] Unlike rigid granular particles, individual microgels are capable of large deformations and volume changes, allowing packing fractions to exceed the random close packing limit of hard spheres.[2,5] Most often, microgels are composed of charged polymers, which strongly drives their swelling and enables the use of extremely long chain lengths between cross-links; most commercially available and laboratory synthesized microgels rely on anionic charge species to promote swelling and achieve jamming at relatively low polymer concentrations.[6−8] While microgels have been used extensively for studying the role of particle elasticity in the glass transition and jamming phenomena,[1,9−11] they remain practically untapped as a biomaterial with limited applications largely focused on drug delivery and cell encapsulation.[12,13]

Recently, jammed microgels have been employed as sacrificial support materials for 3D printing structures made from a diversity of soft matter components including polymers, hydrogels, silicone elastomers, and living cells.[14−18] In contrast to other sacrificial support materials such as polymers with reversible bonds,[19,20] packed micelles,[21] and buoyancy-matched salt solutions,[22,23] jammed granular microgels exhibit solid-like behavior over long time scales, providing stability to 3D-printed structures.[24] When swollen in cell growth media, microgels can be employed as a support material for 3D

Received: December 6, 2018
Accepted: February 26, 2019
Published: February 26, 2019

DOI: 10.1021/acsabm.8b00784
ACS Appl. Bio Mater. 2019, 2, 1509−1517

bioprinting, allowing for controlled, systematic studies of microtissue and tumor development (Figure 1a).[14,25] Alternatively, individual cell behavior may be examined through the dispersion of cells in this 3D cell culture medium (Figure 1b).[26] However, cell culture media contains several monovalent and divalent cations, including Na^+, K^+, Ca^{2+}, and Mg^{2+}, which are involved in numerous cellular processes including cell−cell adhesion, cell signaling, and regulation of internal osmotic pressure.[27] While the sensitivity of charged microgels to added salt is well understood in the case of monovalent ions such as Na^+ and Cl^-,[28−30] the changes in the rheological properties of packed polyelectrolyte microgels in the presence of multivalent ions, such as those within cell growth media, have not been thoroughly investigated. Understanding how multivalent ion−polyelectrolyte interactions influence the rheological properties of microgel systems is necessary to guide the development and application of new microgels for use in biomaterial systems.

Here, we synthesize anionic, cationic, and zwitterionic microgels and systematically investigate the role of multivalent ion−polyelectrolyte interactions on the rheological properties of microgel systems. We design polyelectrolyte microgels with either anionic (MAA), cationic (qDMAEMA), or zwitterionic (CBMA) charged species at varying charge densities and study their changes in rheological properties in the presence of increasing concentrations of Ca^{2+} and Cl^- ions. In the high-salt limit, the rheological behavior of anionic and cationic microgels follow polyelectrolyte scaling laws, while the rheological properties of zwitterionic microgels become independent of added salt. In addition, we explore the application of these polyelectrolyte microgels as biomaterials by culturing cells in microgel environments. Cell performance in the presence of polyelectrolyte microgels is quantified through short-term viability, proliferation, and metabolic activity assays. We find that cell performance is dependent on the chemical composition of the microgels and remains relatively independent of the rheological behavior; anionic and zwitterionic microgels have minimal effect on the short-term viability and metabolic activity of cultured cells, while our cationic microgels appear cytotoxic. Thus, the rheological properties of these jammed microgel packed can be tuned and optimized for bioprinting and 3D cell culturing applications independent of cell performance.

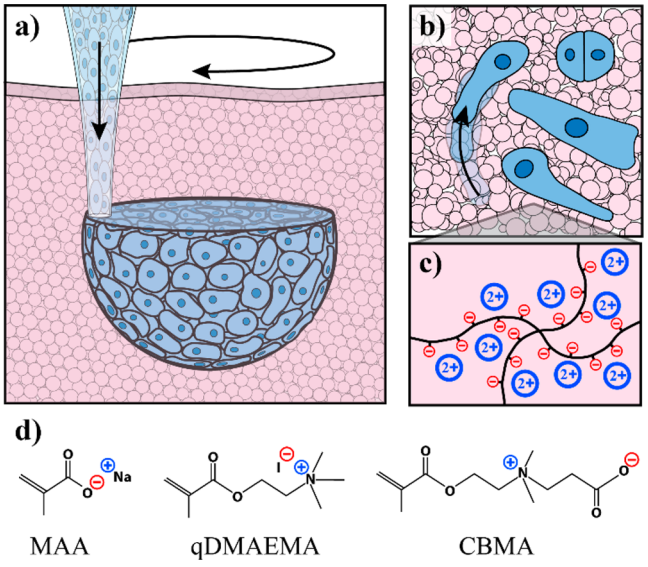

Figure 1. Jammed microgels as a biomaterial. (a) Jammed granular microgels can act as sacrificial support materials for 3D printing cellular constructs, allowing the study of collective cell mechanics and microtissue growth in a controlled 3D environment. (b) Similarly, jammed granular microgels may be used to study the behavior of individual cells in 3D environments. (c) Swelling of charged microgels is driven by the osmotic pressure of counterions associated with polyelectrolyte backbones. (d) Here, we investigate microgel particles containing methacrylic acid (MAA), quaternized 2-(dimethylamino)-ethyl methacrylate (qDMAEMA), or carboxybetaine methacrylate (CBMA) charged monomer species at varying charge densities.

MATERIALS AND METHODS

Microgel Synthesis and Preparation. Cationic, anionic, and zwitterionic microgels are synthesized as previously reported with some modifications.[30] Briefly, a solution of acrylamide (Alfa-Aesar), ionizable comonomer (see below), poly(ethylene glycol) diacrylate (M_n = 700 g mol^{-1}, Sigma-Aldrich), and azobis(isobutyronitrile) (Sigma-Aldrich) in ethanol is prepared. The solution is sparged with nitrogen for 30 min and then placed into a preheated oil bath set at 60 °C. After approximately 30 min, the solution becomes hazy, and a white precipitate begins to form. The reaction mixture is heated for an additional 4 h. At this time, the precipitate is collected by vacuum filtration and rinsed with ethanol on the filter. The microparticles are triturated with 500 mL of ethanol overnight. The solids are collected by vacuum filtration and dried on the filter for ∼10 min. The particles are dried completely in a vacuum oven set at 50 °C to yield a loose white powder. Specific details for the various compositions are included in Table S1.

Anionic microparticles are synthesized using methacrylic acid (Sigma-Aldrich) as comonomer. Zwitterionic microparticles are synthesized using carboxybetaine methacrylate (CBMA). CBMA is synthesized using a modified version of a previously reported procedure.[31] Briefly, DMAEMA (20.0 g) is added to a round-bottom flask equipped with a magnetic stirrer and cooled to 0 °C. Acrylic acid (18.3 g) is added drop-wise at 0 °C, and the mixture is allowed to stir at 0 °C for 30 min, then 4 h at room temperature. At this time, anhydrous tetrahydrofuran (25 mL) is added and the mixture is stirred for 16 h. Triethylamine (25 mL) is added to deprotonate the resulting monomer. Anhydrous THF and anhydrous diethyl ether are added to precipitate the zwitterionic monomer. The monomer is collected by vacuum filtration, dried under vacuum, and stored in a desiccator. Cationic microparticles are synthesized using quaternized 2-(dimethylamino)ethyl methacrylate (qDMAEMA). qDMAEMA is synthesized as previously described.[32] Briefly, DMAEMA (18.7 g) is mixed in anhydrous THF (30 mL). Methyl iodide (20.2 g) in anhydrous THF (30 mL) is added drop-wise at 0 °C. The reaction mixture is warmed to room temperature and stirred for 24 h. At this time, the monomer is collected by vacuum filtration and rinsed on the filter with anhydrous THF. The white solid is dried under vacuum and stored in a desiccator.

Microgel samples are prepared by dispersing the microparticles in ultrapure Millipore water to the desired polymer concentration. Samples are subsequently speed-mixed (FlakTec) and allowed to equilibrate overnight. NaOH is added to the anionic microgels to deprotonate the methacrylic acid charged species until a final pH of ∼6.4 is reached. Calcium chloride dihydrate (Fisher) is added to the microgel solutions to study the effects of ion-polyelectrolyte interactions on the rheological behavior of microgel packs.

Rheology. Rheological measurements are performed on a Malvern Kinexus Pro Rheometer with a 40 mm 1° roughened cone on plate configuration and an Anton Paar MCR 702 Rheometer with a 50 mm, 1.0° cone on plate configuration. Unidirectional shear sweeps are performed by ramping the shear rate from 500 to 10^{-3} s^{-1} and measuring the resulting shear stress. Frequency sweeps are performed at 1% strain from 10 to 10^{-2} Hz using the same geometric configuration.

DOI: 10.1021/acsabm.8b00784
ACS Appl. Bio Mater. 2019, 2, 1509−1517

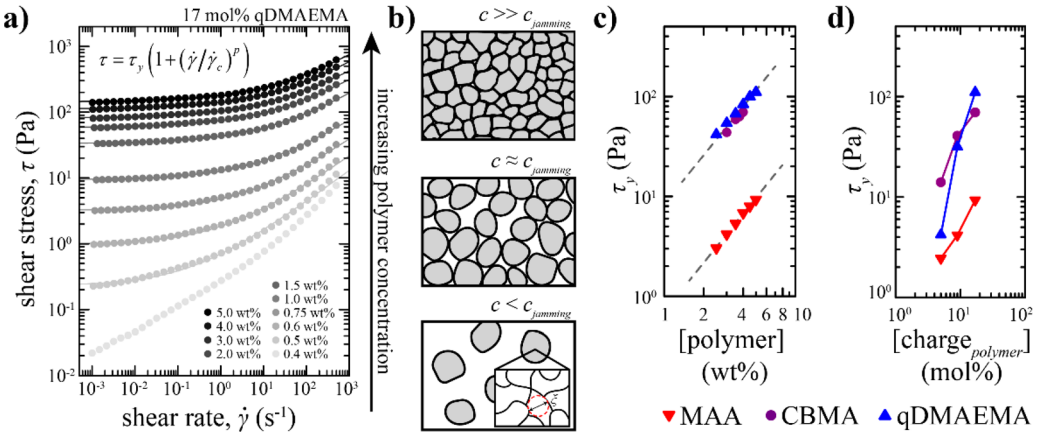

Figure 2. Rheological characterization of charged microgels, (a) Unidirectional shear rate sweeps are performed on microgel samples prepared at increasing polymer concentrations to determine the jamming concentration. (b) In the dilute regime, in which the polymer concentration is below the jamming concentration, the shear stress exhibits a purely viscous response to the applied shear rate. As the polymer concentration increases toward the jamming concentration, the microgel particles become packed, and the system exhibits a finite yield stress. Further increasing the polymer concentration leads to elastic deformation of the microgel particles, enabling the packing factor to exceed that of random close packed hard spheres. The yield stress of microgel packs prepared at concentrations above the jamming concentration is determined by fitting the Hershel–Bulkley model to the data. (c) Increasing the polymer concentration leads to an increase in the measured yield stress for microgels prepared with constant polymer charge density (shown here: 17 mol % charged groups; no added $CaCl_2$; lines drawn to guide the eye). (d) Similarly, the yield stress increases with increasing polymer charge density for microgels prepared at the same polymer concentration (MAA, qDMAEMA: 5 wt % polymer; CBMA: 4 wt %; no added $CaCl_2$). Error bars are smaller than graphical symbols.

Cell Culture and Short-Term Viability. Human mammary epithelial cells (MCF-10A) are cultured in MEBM cell culture medium supplemented with MEGM BulletKit supplements (Lonza) and incubated at 37 °C, 5% CO_2, and 95% humidity. Microgels for cell culturing are swollen in MEGM cell growth media to a final polymer concentration of 4 wt %. NaOH is added to the medium to adjust the pH to 7.4 under incubation conditions. The salt concentrations of MEGM cell growth media are as follows: 2 mM $CaCl_2$, 112 mM NaCl, 2.5 mM KCl, and 1.5 mM $MgSO_4$.

Short-term cell viability assays are performed by dispersing MCF-10A cells in microgel prepared at 4 wt % polymer in MEGM media. After passaging, the cells are pelleted and resuspended at a high density in liquid growth media before subsequently being pipetted into the microgel growth media. The cells and microgels are gently pipet-mixed to evenly disperse the cells throughout the suspension and incubated at 37 °C and 5% CO_2. ReadyProbes Cell Viability Blue/Green Imaging Kit (Thermo Fisher) is added to the microgel media per the manufacturer's instructions at the 3 and 24 h time points and gently pipet-mixed. The cells are then incubated for an additional 30 min before cell viability images are taken using confocal microscopy.

Cell proliferation measurements are performed by plating MCF-10A cells in glass bottomed Petri dishes with liquid growth media. A total of 24 h after plating, cells are dyed with 10 μM CMFDA Cell Tracker Green (Thermo Fisher) for 30 min. After dyeing, cells are culture in liquid cell growth media for 2 h. The liquid media is subsequently replaced with microgel media and cells are incubated at 37 °C and 5% CO_2. Fluorescence images are taken at the 0, 24, and 48 h time points after the microgel media has been introduced. Cell density measurements are determined by counting the number of cells present in the fluorescence images field of view.

Cell Metabolic Activity. Cell metabolic activity studies are performed using CellTiter-Glo 3D Cell Viability Assay (Promega). After passaging, cells are plated in a tissue-treated 96-well plate with liquid cell growth media. Cells are allowed to settle and attached to the well plate for 2 h before the liquid media is replaced with 100 μL of microgel media and cultured for 24 h. After 24 h, 100 μL of CellTiter-Glo 3D assay is added to each well. The media is pipet-mixed and then placed on an orbital shaker for 25 min. After mixing, all 200 μL are transferred to an opaque 96 well plate (Corning), and luminescence measurements are taken on a BioTek Synergy HTX microplate reader. Luminescence calibration curves are performed using known concentrations of adenosine 5′-triphosphate (ATP) disodium salt hydrate (Sigma).

Data Analysis. Confocal scans and fluorescence imaging are performed on a Nikon C2+ confocal microscope. Images are processed in FIJI ImageJ. All data analysis and curve fitting is performed in Origin.

RESULTS AND DISCUSSION

To explore the effects of polyelectrolyte–ion interactions on the rheological properties of jammed granular microgels, we synthesize charged microgels composed of polyacrylamide (pAAm) polymers containing ionized comonomers cross-linked with 1 mol % poly(ethylene glycol) diacrylate (PEGda, M_n = 700 g mol^{-1}) through a precipitation polymerization in ethanol. Each microgel system is prepared with a charged species at varying polymer charge density; here, we use methacrylic acid (MAA) for anionic microgels, quaternized 2-(dimethylamino)ethyl methacrylate (qDMAEMA) for cationic microgels and carboxybetaine methacrylate (CBMA) for zwitterionic microgels (Figure 1d). Phase-contrast micrographs of dilute samples confirm the formation of microgel particles for each of the three charged species explored here (Figure S1). We measure the average size of each microgel in the dilute state and find the mean particle diameters to be 4.76 ± 1.49 μm for MAA microgels, 5.17 ± 1.94 μm for qDMAEMA microgels, and 5.21 ± 2.14 μm for the CBMA microgels (the plus-or-minus intervals correspond to one standard deviation around the mean).

Rheological Characterization. To characterize the rheological properties of our polyelectrolyte microgels, we prepare samples at varying polymer concentration in ultrapure water and record the shear stress response to unidirectional shear rate sweeps (Figure 2a). At polymer concentrations below the jamming concentration, the shear stress exhibits a purely shear-thinning response to an applied stress reflecting dominantly fluid-like behavior (Figure 2a,b). As the polymer concentration is increased above the jamming concentration,

DOI: 10.1021/acsabm.8b00784
ACS Appl. Bio Mater. 2019, 2, 1509–1517

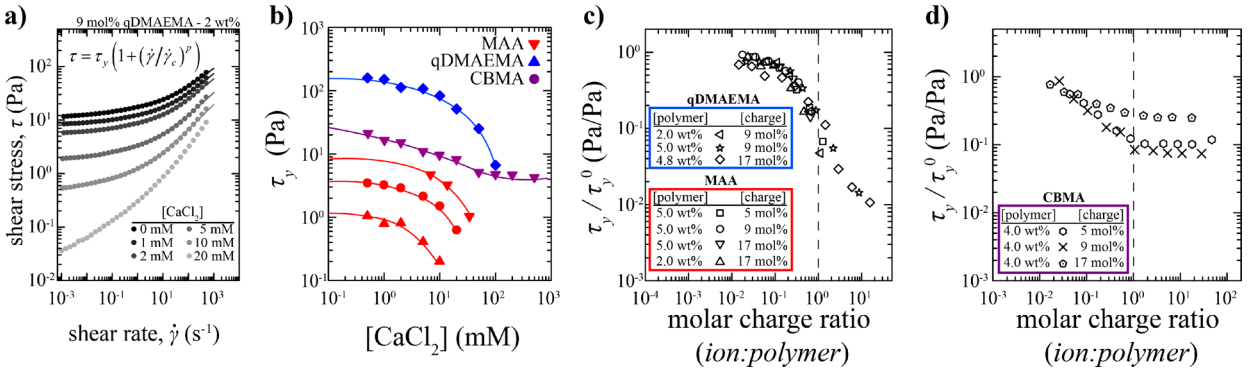

Figure 3. Multivalent ion interactions with charged microgels. (a) Increasing the ionic concentration through the addition of calcium chloride results in a decrease in the measured yield stress; at high ion concentrations, we observe a pure viscous response of the shear stress to the applied shear rate, indicating a transition from the jammed to the dilute regime (shown here: 9 mol % qDMAEMA, 2 wt %). (b) Changes in the rheological behavior are observed for microgels prepared with various charge species, charge densities, and polymer concentrations (shown here: 17 mol % qDMAEMA, 4.8 wt % polymer; 17 mol % CBMA, 4.0 wt % polymer; 17 mol % MAA, 5 wt % polymer; 9 mol % MAA, 5 wt % polymer; 17 mol % MAA, 2 wt % polymer; lines drawn as visual aids). (c) Rescaling the rheological measurements by the yield stress with no added salt and plotting versus the molar charge ratio collapses the data to a single scaling curve for anionic and cationic microgels. (d) Plotting data from zwitterionic microgel systems shows an ion-independent plateau in the rheological properties at molar charge ratios in excess of 1:1. Error bars are smaller than graphical symbols.

the shear stress develops a plateau at low shear rates, which corresponds to the yield stress (Figure 2a,b). This yield stress can be measured by fitting the Hershel−Bulkley model:

$$\tau = \tau_y\left(1 + \left(\frac{\dot\gamma}{\dot\gamma_c}\right)^p\right) \quad (1)$$

to our unidirectional shear rate sweeps, where τ is the measured shear stress, τ_y is the yield stress, $\dot\gamma$ is the applied shear rate, $\dot\gamma_c$ is the cross-over shear rate, and p is a dimensionless constant.[2,33] We find the jamming concentrations of the microgels to be 0.3, 0.45, and 0.9 wt % for microgel particles containing 17 mol % of MAA, qDMAEMA, and CBMA, respectively.

The yield stress of microgel packs may be tuned through changes in either the polymer charge density of the microgels or in the overall polymer concentration. As we increase the polymer charge density at a fixed polymer concentration, the yield stress increases. Likewise, increasing the total polymer concentration results in an increase in the measured yield stress. The shear thinning behavior of jammed microgel packs at high shear rates is captured by the dimensionless constant p in the Hershel−Bulkley model. Here, we find that p covers a range between 0.4 and 0.55, consistent with previously reported values for similar systems.[3] Interestingly, we find that this shear thinning exponent follows a weak logarithmic scaling with the measured yield stress, independent of the monomer charge species present (Figure S2a).

To understand the role of salts on the rheological performance of jammed microgels, we prepare microgel samples with increasing concentrations of calcium chloride, a prevalent multivalent salt in cell growth media. As we increase the ionic charge concentration, we observe a decrease in the measured yield stress; for anionic and cationic microgels prepared with high concentrations of added salt, we observe a purely shear-thinning response to an applied shear rate, suggesting that the system is no longer in a jammed state (Figure 3a). Similar rheological behavior is exhibited in microgels with varying charged species, polymer charge densities, and polymer concentrations (Figure 3b).

To compare rheological behavior across the various samples, we normalize the data by plotting the ratio of the yield stress at a given salt concentration, τ_y, to the yield stress with no added salt, τ_y^0, versus the molar ratio of added ionic charge to polymer charge. For anionic microgels we consider the ionic charge of added Ca^{2+} ions; for cationic microgels, we consider the ionic charge of added Cl^- ions. We find that cationic and anionic microgels collapse to a single curve in which the yield stress decreases with increasing molar charge ratio (Figures 3c and S2b). As the total charge of added ions approaches the number of polymeric charges (molar charge ratio = 1:1), the yield stress decreases to approximately 10% of the initial, zero-salt yield stress, τ_y^0. Further increasing the molar charge ratio leads to a continued decrease in the measured yield stress until a yield stress can no longer be measured and the system exhibits a purely viscous response to an applied shear rate. Surprisingly, zwitterionic microgels exhibit an initial decrease in the measured yield stress followed by a plateau at molar charge ratios greater than 1:1 (Figures 3d and S2c). This initial decrease in measured yield stress with increasing salt concentrations deviates from the anti-polyelectrolyte effect observed in charge neutral polyzwitterions, in which the addition of low-molecular-weight salts results in an increase in swelling.[34] This deviation likely arises from the multivalent nature of Ca^{2+} investigated here.[35] For the cationic and anionic microgels, we investigate the underlying mechanisms that drive the changes in rheological properties with increasing ion concentration by applying polyelectrolyte gel scaling laws to jammed microgel systems, with details given below.

Polyelectrolyte Scaling. Neutral hydrogels swell to an equilibrium concentration in which the driving osmotic pressure (Π) generated from the random motion of the polymer chains is balanced by an elastic restoring force (F_{el}) generated from stretching the polymer chains.[36] In polyelectrolyte hydrogels, dissociated counter-ions near the polymer backbone contribute to the osmotic pressure in addition to the polymeric contribution. When fully swollen, the elastic shear modulus of the polyelectrolyte gel, G', is approximately equal to the osmotic pressure, which can be expressed in terms of a polymeric contribution and an ionic contribution, given by:

DOI: 10.1021/acsabm.8b00784
ACS Appl. Bio Mater. 2019, 2, 1509−1517

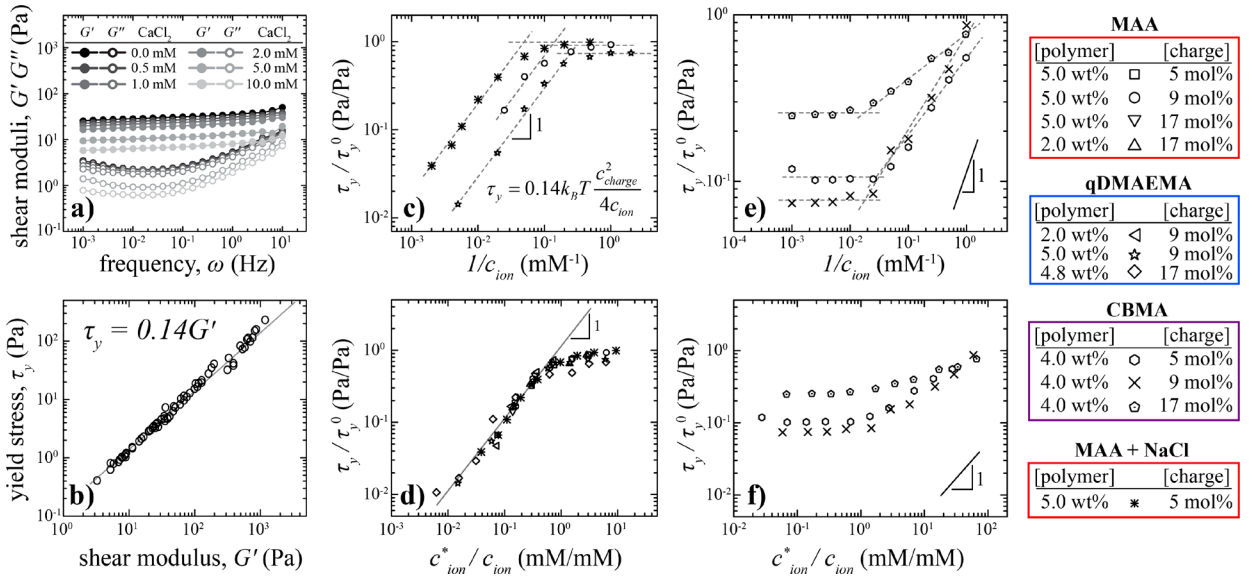

Figure 4. Microgel rheology and polyelectrolyte scaling behavior. (a) The elastic (G') and viscous (G'') shear moduli of the microgels are measured through low-amplitude frequency sweeps. Over a wide range of frequencies, G' remains relatively flat and dominates G'', characteristic of a viscoelastic solid. Increasing the concentration of calcium chloride concentration leads to a decrease in G' and G''. (b) We find the yield stress of microgel packs to be linearly correlated to the elastic shear modulus for all systems under all conditions reported here. (c) To test if polyelectrolyte scaling laws can predict the rheological performance of our anionic and cationic microgels, we plot their normalized yield stress by $1/c_{ion}$. At high concentrations of added salt, the rheological behavior follows the scaling prediction; at low concentrations of added salt, we observe a plateau in the measured yield stress. We identify the critical ion concentration c^*_{ion} in which this transition occurs. (d) Rescaling our rheological curves by c^*_{ion} results in a collapse to a single scaling curve for anionic and cationic microgels. (e) In contrast, the scaling behavior of zwitterionic microgels with the added salt concentration is weaker than the predicted scaling from polyelectrolyte theory and exhibits a plateau at the limits of high amounts of added salt. (f) We find the transition from the weak scaling behavior at low salts and the plateau at high salt levels corresponds to a critical ion concentration comparable to the charge density of the zwitterionic microgels. Error bars are smaller than graphical symbols.

$$G' = k_B T\left(\frac{1}{\xi^3} + \frac{c_p^2}{A(c_p + 4Ac_{ion})}\right) \quad (2)$$

where k_B is the Boltzmann constant, ξ is the polymer mesh-size, c_p is the polymer concentration, A is the average distance between uncondensed charges, and c_{ion} is the concentration of added salt.[37] At the high-salt limit in which $c_p \gg 4Ac_{ion}$, the ionic contribution dominates the polymeric contribution. Here, we assume our polyelectrolyte microgels are fully ionized, and therefore, the ratio of c_p to A can be approximated as the polymer charge concentration (c_{charge}). Thus, at the low-polymer, high-salt limit where the ionic contribution dominates the polymeric contribution, we can simplify this expression to:

$$G' = k_B T\frac{c_{charge}^2}{4c_{ion}} \quad (3)$$

Previous investigations have found polyelectrolyte theory may be applied to microgel systems at concentrations just above jamming.[30] Here, we measure the elastic and viscous shear moduli, G' and G'', of the jammed microgels through low-amplitude frequency sweeps spanning a range between 10^{-3} and 10^{1} Hz (Figure 4a). We find that the elastic component remains relatively flat and dominates the viscous component across the full range of frequencies, consistent with viscoelastic solid behavior. Similar to the yield stress of microgels, the elastic shear modulus decreases with increasing concentrations of calcium chloride. Comparing these two rheological properties, we find that the yield stress of the microgels and the elastic shear modulus at 1 Hz are linearly correlated, such that $\tau_y = 0.14G'$ for all samples exhibiting a yield stress under all conditions reported here (Figure 4b). This relationship between the yield stress and elastic shear modulus of the jammed microgels arises from the elastic energy necessary to deform frictionless particles as they rearrange and slide past one another and is consistent with previous results, indicating that interfacial polymer interactions like entanglements do not dominate yielding in the systems tested here.[30] Thus, we can relate the polyelectrolyte scaling laws for G' to the yield stress of the microgels, given by:

$$\tau_y = 0.14k_B T\frac{c_{charge}^2}{4c_{ion}} \quad (4)$$

To determine if this polyelectrolyte scaling law prediction for added salt applies to jammed granular microgels, we plot the normalized yield stress of the microgels, τ_y / τ_y^0, as a function of the inverse of the ionic charge concentration. In the high-salt limit, where $1/c_{ion}$ is small, we find the normalized yield stress follows the predicted scaling behavior for polyelectrolytes with added salt for both the anionic and cationic microgels at various polymer concentrations and charge densities (Figure 4c). At the low-salt limit, where $1/c_{ion}$ is large, the data deviates from this predicted scaling behavior, and we observe a plateau in the normalized yield stress. We determine a critical ionic charge concentration (c^*_{ion}), in which this transition from the high-salt, polyelectrolyte scaling behavior to the low-salt, plateau regime is observed. Rescaling the rheological curves by c^*_{ion}, we find the data collapses to a single curve in which the yield stress follows polyelectrolyte scaling at high salt concentrations (Figure 4d). This rheological behavior is observed for both the addition of

DOI: 10.1021/acsabm.8b00784
ACS Appl. Bio Mater. 2019, 2, 1509−1517

divalent counterions to anionic microgels (MAA) and monovalent ions to cationic microgels (qDMAEMA). Furthermore, we find the critical ionic charge concentration scales linearly with the charge concentration of the microgel particles and is in close agreement with the limits of the high-salt regime as predicted by polyelectrolyte theory (Figure S3).[37] We further test our hypothesis that the rheological response can be predicted by polyelectrolyte theory by examining anionic microgels in the presence of a monovalent salt (NaCl) and find similar scaling behavior. Similar attempts to rescale the yield stress of zwitterionic microgels do not show the same scaling behavior. At high added salt concentrations, the zwitterionic microgels exhibit a plateau in the yield stress. At low added salt concentrations, the yield stress follows a scaling behavior weaker than that predicted by polyelectrolyte theory (Figure 4e,f).

Previous investigations show that microgels follow polyelectrolyte scaling laws for polymer concentration within a small range of concentrations above jamming.[30] At higher concentrations, jammed microgel behavior deviates from that of fully swollen gels and follows the scaling laws of rubber elasticity.[5,30] Here, we observe similar behavior in our anionic and cationic microgels. As the polymer concentration of the microgels increases above the jamming concentration, individual microgel particles will deform without osmotically driven deswelling, resulting in volume fractions in excess of the random close packing limit of hard spheres.[2,9] However, increasing the concentration of added salts appears to drive the deswelling of the microgel particles, leading to a transition of the system from the jammed to unjammed state. In this limit of high amounts of added salts, the decrease in the ionic contribution to the osmotic pressure can be predicted by polyelectrolyte scaling laws for added salts. We find that this scaling law is dependent on the ionic charge concentration of the added salt and appears independent of the ion valency. Similar behavior has been reported for polyelectrolyte brushes in the presence of mono- and multivalent ions.[38,39] At low salt concentrations, polyelectrolyte brushes are in an "osmotic brush" regime in which the uncondensed counter-ions contribute to the driving osmotic pressure and the brushes maintain an extended configuration; as the concentration of added salts increases, the polyelectrolyte brushes transition to a "salted brush" regime in which a decrease in the osmotic pressure leads to a collapse of the brush structure.[38] Zwitterionic microgel behavior deviates from these polyelectrolyte theory scaling predictions, suggesting the continued contribution to the osmotic pressure, even in the limit of high amounts of added salts.

Cell Viability in Polyelectrolyte Microgels. To explore the applicability of these microgels in biomaterial applications such as 3D bioprinting and 3D cell culture, we investigate the behavior of human mammary epithelial cells (MCF-10A) in microgel packs swollen in cell growth media and determine cell health and performance through measurements of short-term cell viability, cell proliferation rate, and cell metabolic activity. For these experiments, microgel samples are swollen in cell growth media at a polymer concentration of 4 wt %. At these polymer concentrations, all microgels behave like elastic solids when swollen in cell growth media having shear moduli between 2 and 60 Pa (Figure S4). Short-term cell viability measurements are performed on cells dispersed in microgel growth media after 3 and 24 h to determine the population of viable cells (see Figures 5a and S5 and the Materials and Methods section). We find anionic and zwitterionic microgels maintain 90−95% cell viability after 24 h. These results are consistent with previous investigations of cell viability in microgel packs.[14,40] P(qDMAEMA) is a known cytotoxin, often used as an antifouling agent.[41,42] Accordingly, for cells cultured in qDMAEMA microgels we observe increased levels of cell death; while microgels containing 5 mol % qDMAEMA maintain 75% cell viability after 24 h, microgels containing 9 mol % and 17 mol % qDMAEMA exhibit greater than 70% and 90% cell death after 24 h, respectively. While these results demonstrates that microgels containing qDMAEMA do not constitute a suitable cell culture environment, they may find use in biomaterial applications in which targeted cytotoxicity is desired.

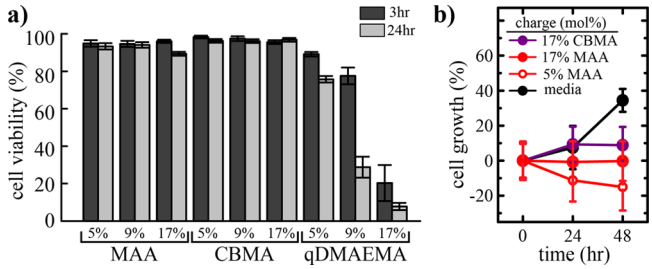

Figure 5. Cell viability and proliferation. (a) Short-term cell viability measurements of MCF-10A suspended in 3D microgel media. Anionic and zwitterionic microgels maintain 90−95% cell viability after 24 h, whereas cells cultured in cationic microgels exhibit increased levels of cell death with increasing charge concentration; cells cultured in 17 mol % qDMAEMA microgels exhibit greater than 90% cell death after 24 h. (b) Relative changes in MCF-10A cell populations cultured in the presence of anionic and zwitterionic microgel media after 24 h are statistically equivalent to liquid culture media (7.5 ± 12.35%). After 48 h, cell population changes in microgels are lower than in liquid media but statistically the same as earlier time-points. (All microgel samples are prepared at 4 wt %; molar concentration of charged species are shown).

Cell Proliferation in Polyelectrolyte Microgels. To investigate cell proliferation in microgel media relative to standard conditions in liquid media, we culture-plated MCF-10A cells in microgel culture media and measure the cell population density at the 0, 24, and 48 h time points (Figures 5b and S6 and the Materials and Methods section). After 24 h, the percent population change of cells cultured in zwitterionic microgel media containing 17 mol % CBMA matched that of liquid media, while both 5 and 17 mol % anionic microgels exhibit a small but statistically insignificant decrease in cell density. We note that this apparent decrease in cell population is consistent with short-term viability results. After 48 h, we observe a considerable deviation in population changes between cells cultured in liquid media and cells cultured in microgel media; cell population changes in microgels are lower than in liquid media but statistically the same as earlier time-points. Fluorescence images of cells cultured in 17 mol % CBMA microgels for 48 h reveal the formation of discrete cell islands similar to those seen in cells cultured in liquid growth media (Figure S6). In contrast, cells cultured in both 5 and 17 mol % MAA form smaller clusters (Figure S6). While this result shows that anionic and zwitterionic microgel media may not suitable for contexts in which cell growth is needed, arresting cell proliferation may be advantageous in applications in which rapid cell growth is undesirable, particularly if cells remain viable and metabolically active. For example, a reduced

DOI: 10.1021/acsabm.8b00784
ACS Appl. Bio Mater. 2019, 2, 1509−1517

proliferation rate may be beneficial in the future when 3D printing tissues with complex vasculature, requiring the precise placement of multiple cell types over long working times.

Metabolic Activity in Polyelectrolyte Microgels. To study how microgel-based biomaterials may affect the metabolic activity of cells, we measure adenosine triphosphate (ATP) levels in MCF-10A cells cultured in microgel media for 24 h using the CellTiter-Glo 3D assay. The CellTiter-Glo 3D assay utilizes a luciferase reaction that produces a luminescence signal proportional to the levels of intracellular ATP.[43] For these experiments, cells are plated into 96-well culture dishes and culture in microgel media for 24 h (Methods).

We perform a series of control experiments to determine the effectiveness of the CellTiter-Glo 3D assay to measure ATP levels in a representative set of our jammed microgel systems. To determine the effectiveness of the luciferase reaction in the microgels, we prepare microgels and liquid media with known concentrations of adenosine 5′-triphosphate disodium salt (Figure 6a). We find the luminescence intensity to be linearly correlated with ATP concentration for our anionic and zwitterionic microgels across the concentration range tested here. Furthermore, the luminescence intensities measured in the microgel media is consistent with the luminescence intensity of ATP measured in liquid cell growth media. These results suggest the luciferase reaction is not hindered by the presence of the polyelectrolyte microgels.

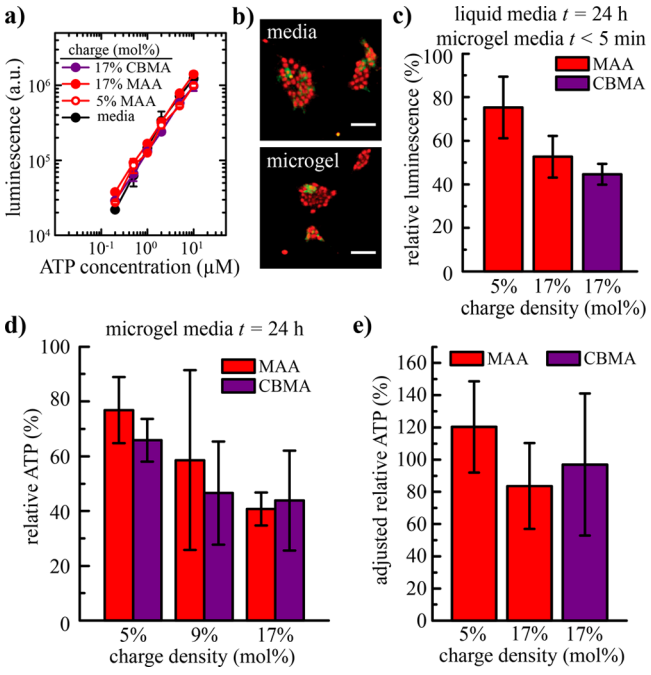

Figure 6. Metabolic activity in polyelectrolyte microgels. (a) CellTiter-Glo 3D calibration measurements of luminescence intensity at known ATP concentrations for liquid and microgel media. (b) Fluorescence microscopy of MCF-10A cultured in microgel media after adding CellTiter-Glo 3D visually confirm cell lysis. [17 mol % MAA; cells dyed Cell Tracker Green CMFDA (green: live) and with ethidium homodimer (red: dead); scale bar: 100 μm.] (c) Relative luminescence intensity of MCF-10A cells cultured in liquid media for 24 h. Liquid media is replaced with microgels immediately prior to cell lysis (t < 5 min). The decrease in luminescence intensity results from microgels hindering the effectiveness of the CellTiter-Glo 3D assay, not a drop in ATP levels. (d) Relative ATP production without correction from MCF-10A cells cultured in microgel media for 24 h relative to cells cultured in liquid media for 24 h. (e) Adjusting the relative ATP levels for the decrease in luminescence intensity (panel c) and accounting for cell proliferation rates (Figure 5b) show no significant change in ATP levels for cells cultured in microgels relative to liquid media. (All microgel samples are prepared at 4 wt %; molar concentration of charged species are shown.)

To test the effectiveness of the assay's detergent in lysing the cells cultured in a microgel environment, we dye MCF-10A cells with Cell Tracker Green CMFDA, a live-cell dye, and culture the cells in microgel media containing 1.1 μM ethidium homodimer, a dead-cell dye that enters the membrane after cell lysis. Fluorescence images taken 30 min after the addition of the CellTiter-Glo 3D assay show an uptake in ethidium homodimer entering the membrane of the cells and a decrease in the CMFDA signal (Figure 6b). These results qualitatively confirm that the CellTiter-Glo 3D detergent successfully lyses the cells in the microgel environment. To quantify the effectiveness of this process, we compare luminescence intensity values of cells cultured in identical conditions but assayed in different media; cells are cultured under identical culture conditions to produce comparable metabolic activity and the microgel culture media is introduced immediately prior to measuring the ATP of the cell (see the Materials and Methods section). Surprisingly, we find a drastic decrease in the luminescence signal produced by the CellTiter-Glo 3D assay in comparison to the signal produced by cells cultured in liquid media (Figure 6c). We find a 25% and 50% decrease in cell luminescence intensity when measured in our 5 and 17 mol % anionic microgels as well as a 55% decrease in intensity when measured in our 17 mol % zwitterionic microgels. These decreases in luminescence intensity occur despite the cells being cultured under identical conditions. Thus, we attribute this decrease in luminescence intensity to the effectiveness of the assay reagents to react with the ATP released by the lysed cells, rather than the cell metabolic activity. Our findings highlight the importance in establishing the proper baseline measurements when developing future assays to measure cell activity in microgel environments.

To explore the changes in metabolic activity of cells in a microgel environment, we culture cells for 24 h in microgels with varying charged species and polymer charge density. We find that the relative luminescence intensity decreases by 30%, 50% and 60% relative to cells cultured in liquid growth media for both the anionic and zwitterionic containing 5, 9, and 17 mol % polymer charge density (Figure 6d). However, when we determine the ATP levels corrected by calibration and the control experiments of luminescence intensity and accounting for proliferation, we find the adjusted relative ATP produced remains statistically unchanged in comparison to liquid growth media (Figure 6e). Thus, we conclude the short-term metabolic activity of MCF-10A cells cultured in the microgel environment is unhindered by the presence of polyelectrolyte. Further studies are needed to investigate the long-term viability and metabolic activity of cells cultured in polyelectrolyte microgels.

CONCLUSIONS

Jammed granular microgels allow for the 3D printing of fluids, polymer solutions, and cells with few constraints on solidification time or rheological properties of the "ink."[14,15] Here, we have designed new polyelectrolyte microgels and characterized their performances as biomaterials for 3D printing and cell culture applications. The rheological proper-

DOI: 10.1021/acsabm.8b00784
ACS Appl. Bio Mater. 2019, 2, 1509−1517

ties of the microgels can be tuned by changing polymer concentration or polymer charge density of the polymeric microparticles. We find that interactions between the polyelectrolyte microgels and ions in the solvent result in a decrease in the ionic contribution to the osmotic swelling of the microgels and consequently drives changes to rheological properties. For anionic and cationic microgels in the high-salt limit, these rheological changes follow the scaling laws describing polyelectrolyte gels with added salt. Further studies on very highly charged polyelectrolyte microgels may be necessary to investigate the effects of salt bridging on their rheological behaviors; the collapse of highly charged polyelectrolyte brushes can be exaggerated in the presence of multivalent ions as a result of electrostatic bridging between chains.[44,45] In contrast, simple polyelectrolyte scaling laws do not capture the rheological behavior of zwitterionic microgels. Instead, zwitterionic microgels exhibit a plateau in rheological properties in the high-salt limit. This unique behavior may be advantageous when swelling microgels in salt-rich solvents, such as cell growth media. However, interactions between the zwitterionic microgels and biological zwitterionic molecules, including amino acids and proteins, may result in unforeseen changes in rheological properties beyond the scope of this work.[46,47] Further development of charge-neutral microgels may circumvent these interactions, providing opportunities for further biomaterial applications using microgels.

We have characterized the performance of MCF-10A cells cultured in charged microgel environments. Short-term viability studies of anionic and zwitterionic microgels showed greater than 90% cell viability after 24 h, while metabolic studies showed that ATP production in the cells remains relatively unchanged. In contrast, cationic microgels containing the qDMAEMA charged species were found to be cytotoxic. These results were independent of the rheological properties of the microgels tested, suggesting that cell performance in jammed microgels is governed by the chemical composition of the microgels and are less sensitive to their rheological properties. Thus, the material properties of the microgels may be tuned to optimize for 3D cell culture or bioprinting applications with limited effects on cell performance. Further assessment is necessary to study the long-term viability of cells cultured in 3D microgel environments. For example, the metabolic activity and hepatic function of in vitro liver constructs are generally characterized through albumin secretion and urea synthesis.[48,49] As new assay protocols are developed to measure these markers of long-term cell function in microgels, proper baselines must be established to account for the effects of the microgel environment.

■ ASSOCIATED CONTENT

Supporting Information

The Supporting Information is available free of charge on the ACS Publications website at DOI: 10.1021/acsabm.8b00784.

A table listing the composition and experimental values for the synthesis of polyelectrolyte microgels; Figures showing phase-contrasted micrographs of dilute microgel samples, additional rheological characterization of polyelectrolyte microgel samples, predicted critical ion concentrations of polyelectrolyte theory, the rheological performance of polyelectrolyte microgels swollen in cell growth media, and representative fluorescence images from short term cell viability studies. (PDF)

■ AUTHOR INFORMATION

Corresponding Author

*E-mail: t.e.angelini@ufl.edu.

ORCID

Christopher S. O'Bryan: 0000-0003-0852-6085
Christopher P. Kabb: 0000-0002-5125-2705
Brent S. Sumerlin: 0000-0001-5749-5444
Thomas E. Angelini: 0000-0002-0313-4341

Notes

The authors declare no competing financial interest.

■ ACKNOWLEDGMENTS

The authors thank Anton Paar for the use of the Anton Paar 702 rheometer through their VIP academic research program. This work was supported by the National Science Foundation under grant nos. DMR-1352043 and DMR-1606410.

■ REFERENCES

(1) Mattsson, J.; Wyss, H. M.; Fernandez-Nieves, A.; Miyazaki, K.; Hu, Z.; Reichman, D. R.; Weitz, D. A. Soft Colloids Make Strong Glasses. *Nature* **2009**, *462* (7269), 83.

(2) Nordstrom, K. N.; Verneuil, E.; Arratia, P.; Basu, A.; Zhang, Z.; Yodh, A. G.; Gollub, J. P.; Durian, D. J. Microfluidic Rheology of Soft Colloids Above and Below Jamming. *Phys. Rev. Lett.* **2010**, *105* (17), 175701.

(3) Pellet, C.; Cloitre, M. The Glass and Jamming Transitions of Soft Polyelectrolyte Microgel Suspensions. *Soft Matter* **2016**, *12* (16), 3710−3720.

(4) Heyes, D.; Brańka, A. Interactions Between Microgel Particles. *Soft Matter* **2009**, *5* (14), 2681−2685.

(5) Menut, P.; Seiffert, S.; Sprakel, J.; Weitz, D. A. Does Size Matter? Elasticity of Compressed Suspensions of Colloidal-and Granular-Scale Microgels. *Soft Matter* **2012**, *8* (1), 156−164.

(6) Saunders, B. R.; Laajam, N.; Daly, E.; Teow, S.; Hu, X.; Stepto, R. Microgels: From Responsive Polymer Colloids to Biomaterials. *Adv. Colloid Interface Sci.* **2009**, *147*, 251−262.

(7) Carl, J. L. I.; Amjad, Z.; III Masler, W. F.; Wingo, W. H. Easy to Disperse Polycarboxylic Acid Thickeners. US Patent 5,288,814, February 22, 1994.

(8) O'Bryan, C. S.; Bhattacharjee, T.; Marshall, S. L.; Sawyer, W. G.; Angelini, T. E. Commercially Available Microgels for 3D Bioprinting. *Bioprinting* **2018**, *11*, 1.

(9) Cloitre, M.; Borrega, R.; Monti, F.; Leibler, L. Glassy Dynamics and Flow Properties of Soft Colloidal Pastes. *Phys. Rev. Lett.* **2003**, *90* (6), No. 068303.

(10) Pelton, R.; Chibante, P. Preparation of Aqueous Latices with N-isopropylacrylamide. *Colloids Surf.* **1986**, *20* (3), 247−256.

(11) Pusey, P. N.; Van Megen, W. Phase Behaviour of Concentrated Suspensions of Nearly Hard Colloidal Spheres. *Nature* **1986**, *320* (6060), 340.

(12) Jiang, Y.; Chen, J.; Deng, C.; Suuronen, E. J.; Zhong, Z. Click Hydrogels, Microgels and Nanogels: Emerging Platforms for Drug Delivery and Tissue Engineering. *Biomaterials* **2014**, *35* (18), 4969−4985.

(13) Oh, J. K.; Drumright, R.; Siegwart, D. J.; Matyjaszewski, K. The Development of Microgels/Nanogels for Drug Delivery Applications. *Prog. Polym. Sci.* **2008**, *33* (4), 448−477.

(14) Bhattacharjee, T.; Gil, C. J.; Marshall, S. L.; Urueña, J. M.; O'Bryan, C. S.; Carstens, M.; Keselowsky, B.; Palmer, G. D.; Ghivizzani, S.; Gibbs, C. P.; et al. Liquid-Like Solids Support Cells in 3D. *ACS Biomater. Sci. Eng.* **2016**, *2* (10), 1787−1795.

(15) Bhattacharjee, T.; Zehnder, S. M.; Rowe, K. G.; Jain, S.; Nixon, R. M.; Sawyer, W. G.; Angelini, T. E. Writing in the Granular Gel Medium. *Sci. Adv.* **2015**, *1* (8), No. e1500655.

(16) O'Bryan, C. S.; Bhattacharjee, T.; Hart, S.; Kabb, C. P.; Schulze, K. D.; Chilakala, I.; Sumerlin, B. S.; Sawyer, W. G.; Angelini, T. E.

DOI: 10.1021/acsabm.8b00784
ACS Appl. Bio Mater. 2019, 2, 1509−1517

Self-Assembled Micro-Organogels for 3D Printing Silicone Structures. *Sci. Adv.* **2017**, *3* (5), No. e1602800.
(17) Kabb, C. P.; O'Bryan, C. S.; Deng, C. C.; Angelini, T. E.; Sumerlin, B. S. Photoreversible Covalent Hydrogels for Soft-Matter Additive Manufacturing. *ACS Appl. Mater. Interfaces* **2018**, *10* (19), 16793−16801.
(18) Hinton, T. J.; Jallerat, Q.; Palchesko, R. N.; Park, J. H.; Grodzicki, M. S.; Shue, H.-J.; Ramadan, M. H.; Hudson, A. R.; Feinberg, A. W. Three-Dimensional Printing of Complex Biological Structures by Freeform Reversible Embedding of Suspended Hydrogels. *Sci. Adv.* **2015**, *1* (9), No. e1500758.
(19) Highley, C. B.; Rodell, C. B.; Burdick, J. A. Direct 3D Printing of Shear-Thinning Hydrogels into Self-Healing Hydrogels. *Adv. Mater.* **2015**, *27* (34), 5075−5079.
(20) Song, K. H.; Highley, C. B.; Rouff, A.; Burdick, J. A. Complex 3D-Printed Microchannels within Cell-Degradable Hydrogels. *Adv. Funct. Mater.* **2018**, *28*, 1801331.
(21) Wu, W.; DeConinck, A.; Lewis, J. A. Omnidirectional Printing of 3D Microvascular Networks. *Adv. Mater.* **2011**, *23* (24), H178−H183.
(22) Landers, R.; Hübner, U.; Schmelzeisen, R.; Mülhaupt, R. Rapid Prototyping of Scaffolds Derived from Thermoreversible Hydrogels and Tailored for Applications in Tissue Engineering. *Biomaterials* **2002**, *23* (23), 4437−4447.
(23) Xu, C.; Chai, W.; Huang, Y.; Markwald, R. R. Scaffold-Free Inkjet Printing of Three-Dimensional Zigzag Cellular Tubes. *Biotechnol. Bioeng.* **2012**, *109* (12), 3152−3160.
(24) O'Bryan, C. S.; Bhattacharjee, T.; Niemi, S. R.; Balachandar, S.; Baldwin, N.; Ellison, S. T.; Taylor, C. R.; Sawyer, W. G.; Angelini, T. E. Three-Dimensional Printing with Sacrificial Materials for Soft Matter Manufacturing. *MRS Bull.* **2017**, *42* (8), 571−577.
(25) Scott, E. A.; Nichols, M. D.; Kuntz-Willits, R.; Elbert, D. L. Modular Scaffolds Assembled Around Living Cells Using poly (ethylene glycol) Microspheres with Macroporation via a Non-Cytotoxic Porogen. *Acta Biomater.* **2010**, *6* (1), 29−38.
(26) Bhattacharjee, T.; Angelini, T. E. 3D T Cell Motility in Jammed Microgels. *J. Phys. D: Appl. Phys.* **2019**, *52* (2), No. 024006.
(27) Ham, R. G.; McKeehan, W. L. Media and Growth Requirements. *Methods Enzymol.* **1979**, *58*, 44−93.
(28) Fernández-Nieves, A.; Fernández-Barbero, A.; De las Nieves, F. Salt Effects Over the Swelling of Ionized Mesoscopic Gels. *J. Chem. Phys.* **2001**, *115* (16), 7644−7649.
(29) López-León, T.; Ortega-Vinuesa, J. L.; Bastos-González, D.; Elaïssari, A. Cationic and Anionic poly (N-isopropylacrylamide) Based Submicron Gel Particles: Electrokinetic Properties and Colloidal Stability. *J. Phys. Chem. B* **2006**, *110* (10), 4629−4636.
(30) Bhattacharjee, T.; Kabb, C. P.; O'Bryan, C. S.; Urueña, J. M.; Sumerlin, B. S.; Sawyer, W. G.; Angelini, T. E. Polyelectrolyte Scaling Laws for Microgel Yielding near Jamming. *Soft Matter* **2018**, *14* (9), 1559−1570.
(31) Li, Y.; Xue, H.; Song, Y., Production and Purification of Carboxylic Betaine Zwitterionic Monomers. US Patent 2014/0275614 A1, September 18, 2014.
(32) Semsarilar, M.; Ladmiral, V.; Blanazs, A.; Armes, S. Cationic Polyelectrolyte-Stabilized Nanoparticles via RAFT Aqueous Dispersion Polymerization. *Langmuir* **2013**, *29* (24), 7416−7424.
(33) Herschel, W. H.; Bulkley, R. Konsistenzmessungen von Gummi-Benzollösungen. *Colloid Polym. Sci.* **1926**, *39* (4), 291−300.
(34) Lowe, A. B.; McCormick, C. L. Synthesis and Solution Properties of Zwitterionic Polymers. *Chem. Rev.* **2002**, *102* (11), 4177−4190.
(35) de Grooth, J.; Ogieglo, W.; de Vos, W. M.; Gironès, M.; Nijmeijer, K.; Benes, N. E. Swelling Dynamics of Zwitterionic Copolymers: The Effects of Concentration and Type of Anion and Cation. *Eur. Polym. J.* **2014**, *55*, 57−65.
(36) Flory, P. J. *Principles of Polymer Chemistry*; Cornell University Press: Ithaca, NY, 1953.
(37) Rubinstein, M.; Colby, R. H.; Dobrynin, A. V.; Joanny, J.-F. Elastic Modulus and Equilibrium Swelling of Polyelectrolyte Gels. *Macromolecules* **1996**, *29* (1), 398−406.
(38) Farina, R.; Laugel, N.; Pincus, P.; Tirrell, M. Brushes of Strong Polyelectrolytes in Mixed Mono-and Tri-valent Ionic Media at Fixed Total Ionic Strengths. *Soft Matter* **2013**, *9* (44), 10458−10472.
(39) Yu, J.; Mao, J.; Yuan, G.; Satija, S.; Chen, W.; Tirrell, M. The Effect of Multivalent Counterions to the Structure of Highly Dense Polystyrene Sulfonate Brushes. *Polymer* **2016**, *98*, 448−453.
(40) Nguyen, P. K.; Snyder, C. G.; Shields, J. D.; Smith, A. W.; Elbert, D. L. Clickable Poly (ethylene glycol)-Microsphere-Based Cell Scaffolds. *Macromol. Chem. Phys.* **2013**, *214* (8), 948−956.
(41) Jones, R. A.; Poniris, M. H.; Wilson, M. R. pDMAEMA Is Internalised by Endocytosis but Does Not Physically Disrupt Endosomes. *J. Controlled Release* **2004**, *96* (3), 379−391.
(42) Álvarez-Paino, M.; Muñoz-Bonilla, A.; López-Fabal, F. t.; Gómez-Garcés, J. L.; Heuts, J. P.; Fernández-García, M. Effect of Glycounits on the Antimicrobial Properties and Toxicity Behavior of Polymers Based on Quaternized DMAEMA. *Biomacromolecules* **2015**, *16* (1), 295−303.
(43) Hannah, R.; Beck, M.; Moravec, R.; Riss, T. CellTiter-Glo Luminescent Cell Viability Assay: A Sensitive and Rapid Method for Determining Cell Viability. *Promega Cell Notes* **2001**, *2*, 11−13.
(44) Farina, R.; Laugel, N.; Yu, J.; Tirrell, M. Reversible Adhesion with Polyelectrolyte Brushes Tailored via the Uptake and Release of Trivalent Lanthanum Ions. *J. Phys. Chem. C* **2015**, *119* (26), 14805−14814.
(45) Brettmann, B. K.; Laugel, N.; Hoffmann, N.; Pincus, P.; Tirrell, M. Bridging Contributions to Polyelectrolyte Brush Collapse in Multivalent Salt Solutions. *J. Polym. Sci., Part A: Polym. Chem.* **2016**, *54* (2), 284−291.
(46) Vaisocherova, H.; Yang, W.; Zhang, Z.; Cao, Z.; Cheng, G.; Piliarik, M.; Homola, J.; Jiang, S. Ultralow Fouling and Functionalizable Surface Chemistry Based on a Zwitterionic Polymer Enabling Sensitive and Specific Protein Detection in Undiluted Blood Plasma. *Anal. Chem.* **2008**, *80* (20), 7894−7901.
(47) Zhang, Z.; Chen, S.; Jiang, S. Dual-Functional Biomimetic Materials: Nonfouling poly (carboxybetaine) with Active Functional Groups for Protein Immobilization. *Biomacromolecules* **2006**, *7* (12), 3311−3315.
(48) Shulman, M.; Nahmias, Y. Long-Term Culture and Coculture of Primary Rat and Human Hepatocytes. In *Epithelial Cell Culture Protocols*; Springer: New York, NY, 2012; pp 287−302.
(49) Sistare, F. D.; Mattes, W. B.; LeCluyse, E. L. The Promise of New Technologies to Reduce, Refine, or Replace Animal Use While Reducing Risks of Drug Induced Liver Injury in Pharmaceutical Development. *ILAR J.* **2016**, *57* (2), 186−211.

DOI: 10.1021/acsabm.8b00784
ACS Appl. Bio Mater. 2019, 2, 1509−1517

Supporting Information

Jammed Polyelectrolyte Microgels for 3D Cell Culture Applications: Rheological Behavior with Added Salts

Christopher S. O'Bryan,[a] Christopher P. Kabb,[b] Brent S. Sumerlin,[b] Thomas E. Angelini [a,c,d,e,*]

[a] Department of Mechanical & Aerospace Engineering, Herbert Wertheim College of Engineering, University of Florida, Gainesville, Florida 32611, United States
[b] George & Josephine Butler Polymer Research Laboratory, Center for Macromolecular Science & Engineering, Department of Chemistry, University of Florida, Gainesville, Florida 32611, United States
[c] J. Crayton Pruitt Family Department of Biomedical Engineering, University of Florida Herbert Wertheim College of Engineering, Gainesville, Florida 32611, United States
[d] Institute for Cell & Tissue Science and Engineering, University of Florida, Gainesville, Florida 32611, United States
[e] Department of Materials Science and Engineering, Herbert Wertheim College of Engineering, University of Florida, Gainesville, Florida 32611, United States
* Corresponding Author: t.e.angelini@ufl.edu

Supplemental Material

Comonomer	Comonomer Incorporation (mol %)	AAm (g)	Comonomer (g)	$PEG_{700}da$ (g)	AIBN (mg)	EtOH (mL)
MAA	5	8.55	0.55	0.90	100	112
MAA	9	8	1	1	100	112
MAA	17	7.27	1.82	0.91	100	112
CBMA	5	7.85	1.33	0.82	100	112
CBMA	9	7.01	2.23	0.76	100	112
CBMA	17	5.59	3.74	0.67	100	112
qDMAEMA	5	7.52	7.69	0.79	100	112
qDMAEMA	9	6.54	2.75	0.71	100	112
qDMAEMA	17	5.02	4.38	0.60	100	112

Table S1 – Experimental values for the synthesis of 10g of polyelectrolyte microgels composed of polyacrylamide with anionic (MAA), zwitterionic (CBMA), and cationic (qDMAEMA) comonomers.

Phase Contrasted Micrographs of Dilute Microgel Samples

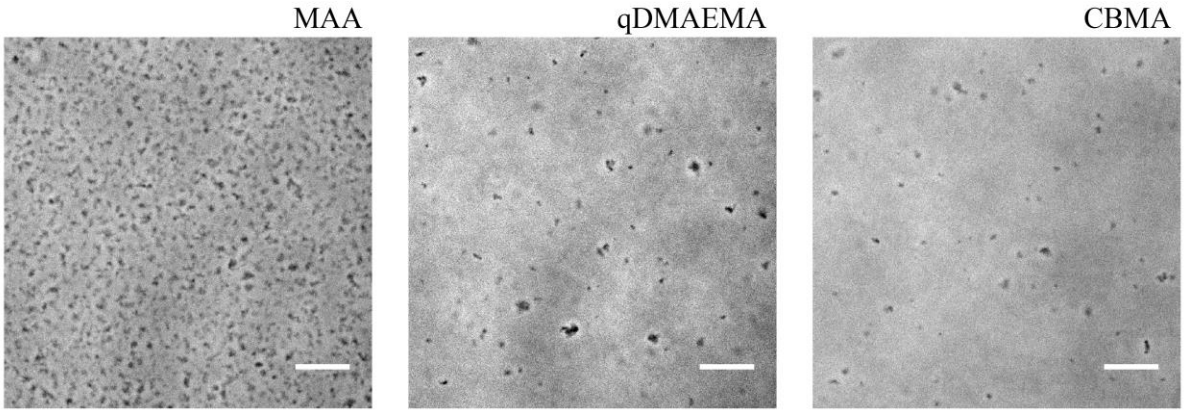

Figure S1 – Phase contrasted micrographs of dilute samples confirm the presence of anionic (MAA), cationic (qDMAEMA), and zwitterionic (CBMA) microgels. We measure the average size of each microgel in the dilute state and find the mean particle diameters to be 4.76±1.49 μm for MAA microgels, 5.17±1.94 μm for qDMAEMA microgels, and 5.21±2.14 μm for the CBMA microgels. Scale bar: 200 μm

Polyelectrolyte Microgel Rheology

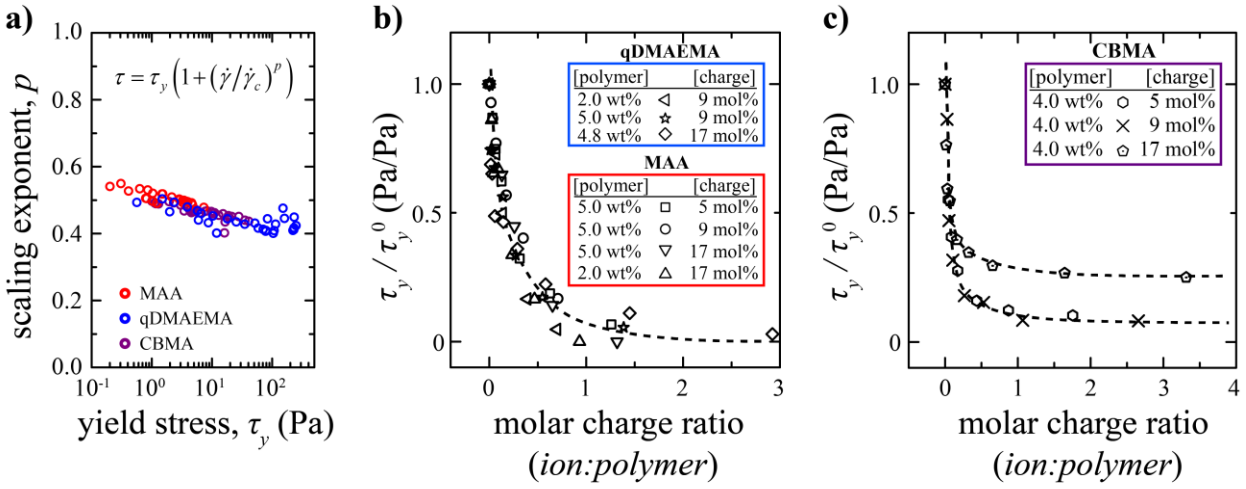

Figure S2 – Rheological Characterization of Polyelectrolyte Microgels: **a)** The yield stress of microgel samples is measured by fitting the Hershel-Bulkley model, $\tau = \tau_y\left(1 + \left(\dot{\gamma}/\dot{\gamma}_c\right)^p\right)$, to unidirectional shear rate sweeps. Here we find that the scaling exponent p falls between 0.4 and 0.55, indicating shear thinning behavior at high shear rates. Interestingly, this scaling exponent follows a weak logarithimic scaling with the measured yield stress. b) To compare rheological results of microgels with added salt across samples, we plot the ratio of the yield stress at a given salt concentration to the yield stress with no added salt (τ_y / τ_y^0) as a function of the molar ratio of added ionic charge to polymer charge. The rheological results for anionic and cationic microgels collapse to a single curve in which the yield stress decreases with increasing salt concentrations. At high molar charge ratios, the microgels exhibit a purely viscous response to an applied shear rate and the yield stress is 0. **c)** Zwitterionic microgels exhibit an initial, steeper collapse followed by a non-zero plateau in the measured yield stress at high salt concentrations.

High Salt Prediction for Anionic and Cationic Microgels.

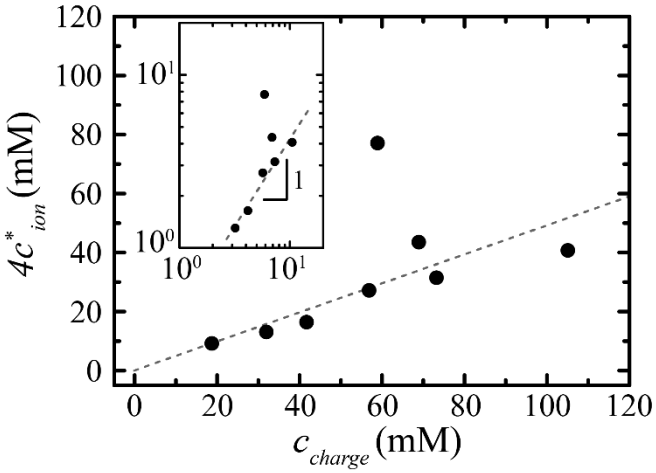

Figure S3 – The critical ion charge concentration scales linearly with the charge concentration of the microgel particles and is in close agreement with the limits of the high-salt regime as predicted by polyelectrolyte theory, i.e. $c_{charge} << 4c_{ion}$.

Microgel Rheology in MEGM Cell Growth Media.

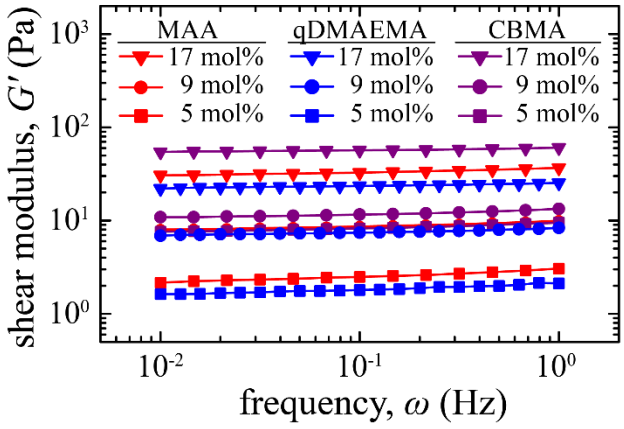

Figure S4 – Small amplitude oscillatory frequency sweeps of polyelectrolyte microgels swollen in MEGM cell growth media at 4 wt % polymer. The elastic shear modulus (G') remains relatively flat across the full range of frequencies, confirming the microgels are in the jammed state and ranges from 2 – 60 Pa.

Cell Viability in Polyelectrolyte Microgels

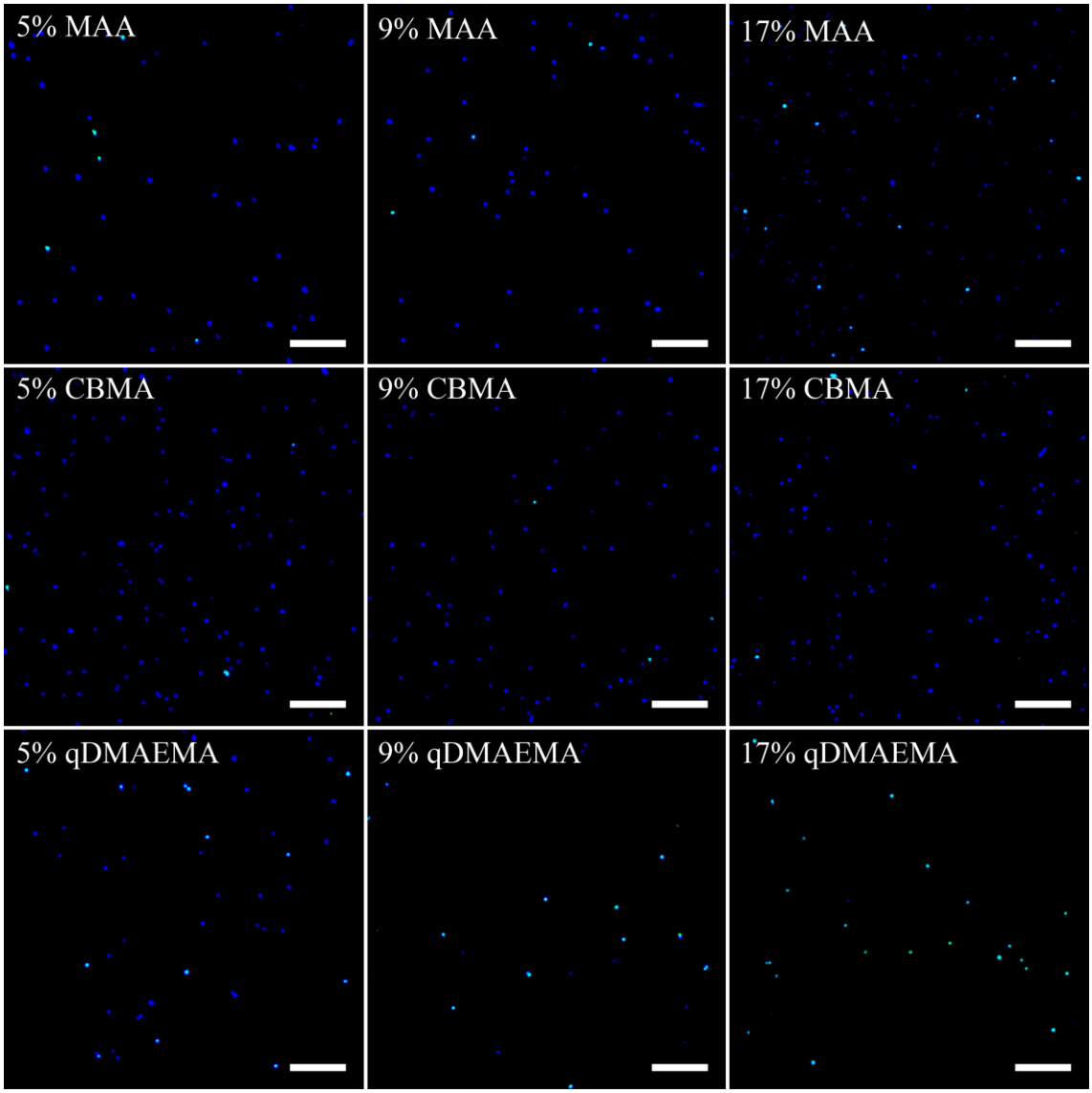

Figure S5 – Short-term cell viability measurements of MCF-10A cells suspended in jammed polyelectrolyte microgels for 24 hours are performed using ReadyProbes Blue/Green cell viability imaging kit. Microgel samples are prepared at 4 wt % polymer with varying charge species and charge densities. Shown here are representative max intensity projections of fluorescence confocal microscopy scans taken after 24 h of culture. Cell viability is determined by counting the total cell population (blue) and the number of dead cells (green). Anionic (MAA) and zwitterionic (CBMA) microgels maintain 90-95% cell viability after 24 h whereas cells cultured in 17 mol % qDMAEMA microgels experience greater than 90% cell death after 24 hours. Scale bars: 200 μm.

Cell Proliferation Fluorescence Images

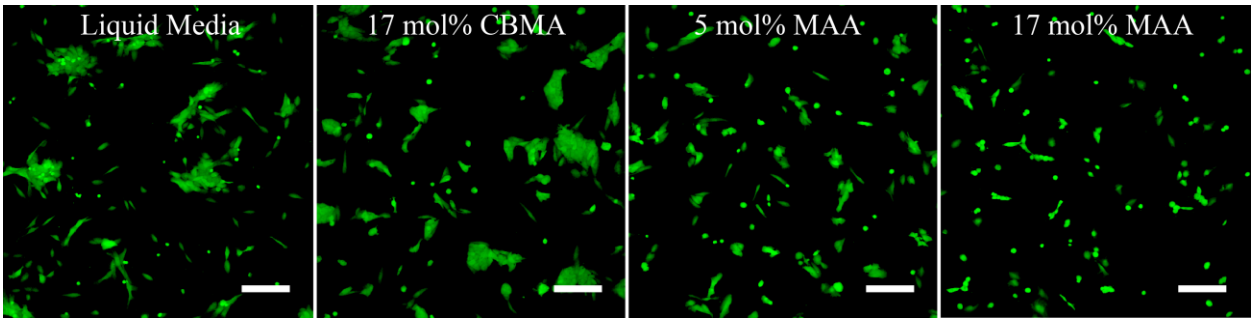

Figure S6 – Fluorescence microscopy images of MCF-10A cells cultured in jammed polyelectrolyte microgels. MCF-10A cells are dyed with CMFDA cell tracker green, plated on a glass bottom 12-well plates and cultured in microgel support media. Cell population growth rates from the cell population density determined by counting the number of cells for a given culture area. Scale bar: 200 μm.